Histol Histopathol (2014) 29: 1565-1573
DOI: 10.14670/HH-29.1565

http://www.hh.um.es

Histology and Histopathology
Cellular and Molecular Biology

Nestin and WT1 expression in atheromatous plaque neovessels: association with vulnerability

Silvia Fittipaldi[1]*, Francesco Vasuri[1,2]*, Alessio Degiovanni[2], Rodolfo Pini[1], Raffaella Mauro[1], Gianluca Faggioli[1], Antonia D'Errico-Grigioni[2], Andrea Stella[1] and Gianandrea Pasquinelli[2]

[1]Unit of Vascular Surgery, Department of Specialty, Diagnostic and Experimental Medicine (DIMES), S.Orsola-Malpighi Hospital, Bologna University and [2]Unit of Surgical Pathology, Department of Specialty, Diagnostic and Experimental Medicine (DIMES), S.Orsola-Malpighi Hospital, Bologna University, Bologna, Italy

*S.F. and F.V. equally contributed to the paper

Summary. Introduction. Neoangiogenesis is crucial for the progression and vulnerability of atheromasic lesions. Since adult *vasa vasorum*, which represent the neoangiogenetic burden of healthy arteries, constitutively express Nestin and Wilms Tumor (WT1), the aims of the present study are: i) to describe and quantify Nestin and WT1 in plaque neovessels; ii) to investigate the relationship between neovessel phenotype and plaque instability.

Methods. We prospectively evaluated 49 consecutive carotid endarterectomy specimens. Histopathological characteristics were separately collected, particularly the intraplaque histological complications. Immunohistochemistry was carried out for CD34, Nestin and WT1; the density of positivity was evaluated for each marker. RT-PCR was performed to assess Nestin and WT1 mRNA levels on the first 10 plaques and on 10 control arteries.

Results. Six (12.2%) plaques showed no neoangiogenesis. In the others, the mean immunohistochemical densities of CD34, Nestin, and WT1-positive structures were 41.88, 28.84 and 17.68/mm^2. Among the CD34+ neovessels, 68% and 42% expressed Nestin and WT1 respectively, i.e., nearly 36% of the neovessels resulted to be Nestin+/WT1-. Furthermore, complicated plaques (n=30) showed significantly more CD34 and Nestin-positive vessels than uncomplicated plaques (n=13; P=0.045 and P=0.009), while WT1 was not increased (P=0.139). RT-PCR confirmed that WT1 gene expression was 3-fold lower than Nestin gene in plaques (p=0.001).

Conclusions. Plaque neoangiogenesis shows both a Nestin+/WT1- and a Nestin+/WT1+ phenotype. The Nestin+/WT1- neovessels are significantly more abundant in complicated (vulnerable) plaques. The identification of new transcription factors in plaque neoangiogenesis, and their possible regulation, can open new perspectives in the therapy of vulnerable plaques.

Key words: Atherosclerosis, Nestin, WT1, Histopathology, RT-PCR.

Offprint requests to: Gianandrea Pasquinelli, Unit of Surgical Pathology, Department of Specialty, Diagnostic and Experimental Medicine (DIMES), S.Orsola-Malpighi Hospital, via Massarenti 9, 40138 Bologna, Italy. e-mail: gianandr.pasquinelli@unibo.it

Introduction

The vulnerable plaques had been initially characterized by a large lipid core, a thin fibrous cap, a rich infiltrate of macrophages and scarce smooth muscle cells (Kullo et al., 1998). More recently, neoangiogenesis was defined as one of the most important pathological processes involved in the progression of atheromasic lesions (Hermus et al., 2010). Indeed, neovessel formation has been related to an increased plaque vulnerability and to the onset of symptomatic plaques (Mofidi et al., 2001; Faggioli et al., 2011). The neovessel density is directly related with plaque growth and progression (Moreno et al., 2006), but also the morphology of the neoangiogenetic structures influences the plaque stability. It has been shown that plaque neovessels lack extracellular junctions (Sluimer et al., 2009), and that the neovessels of

symptomatic plaques are larger and more irregular compared to the neovessels of asymptomatic plaques (McCarthy et al., 1999).

Since it was demonstrated that plaque neovessels originate mainly from adventitial *vasa vasorum* (Kumamoto et al., 1995), we recently focused on the *vasa vasorum* phenotype and neoangiogenetic potential in healthy arteries. In particular, we observed that adult *vasa vasorum* express Nestin and the transcription factor Wilms Tumor 1 (WT1) (Vasuri et al., 2012). WT1 is normally expressed during embryogenesis (Wagner et al., 2006), and recent findings showed its importance in heart and coronary vessel development (Scholz et al., 2009). Nevertheless, WT1 was also detected in a variety of human tumors, and in tumoral neoangiogenesis (Hohenstein and Hastie, 2006; Wagner et al., 2008). Furthermore, recent studies showed the involvement of WT1 as an activator of the Nestin gene (Hohenstein and Hastie, 2006). Nestin, an intermediate filament protein expressed by a variety of progenitor cells (Wagner et al., 2006), was originally also described as a marker of newly forming blood vessels during tumoral and not-tumoral neoangiogenesis (Teranishi et al., 2007; Ramasamy et al., 2011). Our recent experience indicates that WT1 and Nestin colocalize with a 1:1 ratio in the *vasa vasorum* endothelium from adult healthy arteries (Vasuri et al., 2012).

No studies have been performed on the expression of WT1 and Nestin in the neoangiogenetic component of the atheromatous plaques yet. The aims of this study are: i) to describe and quantify the immunomorphological features and mRNA levels of WT1 and Nestin in the plaque neovessels; ii) to investigate the role of neovessel phenotype in the occurrence of the histological complications correlated with plaque instability.

Materials and methods

Case selection

We prospectively evaluated 49 consecutive patients (34 males and 15 females; mean age at surgery 71.4 ±8.1 years, range 48-86 years) over a 2-year time length. According to the recommendations from the European Society for Vascular Surgery (ESVS) and the Society of Vascular Surgeons (SVS) (Hobson et al., 2008; Liapis et al., 2009), the indications for carotid endarterectomy (CEA) included: plaques with stenosis ≥70% (independently on the presence of symptoms), or symptomatic carotid plaques with stenosis ≥50%. Symptomatic carotid stenosis was defined as the occurrence of ipsilateral cerebral ischemic events (major or minor stroke, transient ischemic attack, or amaurosis fugax) in the last 6 months.

To compare Nestin and WT1 mRNA levels of expression, we also selected the first 10 plaque cases of our series and 10 specimens from normal arteries as controls, collected from the Cardiovascular Tissue Bank of S.Orsola-Malpighi Hospital of Bologna (Vasuri et al., 2012).

Histopathological analysis

Carotid plaques were fully removed during surgery to preserve the plaque structure. At gross examination, samples were cut in serial sections to identify the areas with stenosis or macroscopic complications (i.e. erosions, hemorrhages, ulcerations). Plaque tissue was therefore sampled *in toto*, fixed in formalin buffered 4% and embedded in paraffin. Two-μm-thick sections were cut for haematoxylin and eosin stain and immunohistochemistry (IHC). Histopathological characteristics were blindly collected by two experienced pathologists. The histological parameters collected included: the maximum and minimum fibrous cap thickness, the extension of the lipid core, the occurrence of calcifications, the amount of macrophagic/lymphocytic infiltrate (assessed as absent, mild, moderate, or severe/diffuse), the amount of neoangiogenesis (absent, focal, moderate, or diffuse). The presence or absence of complications in the plaques, and therefore the classification according to the American Heart Association (AHA) (Stary et al., 1995; Stary, 2000), were evaluated as well.

The 10 normal vascular specimens used for RT-PCR were fixed and processed as for the plaque specimens: histopathological analysis showed no relevant pathological alterations in these samples.

Immunohistochemical assay

Formalin-fixed paraffin embedded (FFPE) 2-μm-thick sections were rehydrated through graded steps of ethanol absolute (Xylol 30min, 100% 10 min, 95% 5 min, 70% 5 min). Immunostainings for CD34 and WT1 were automatically performed with Benchmark ULTRA® immunostainer (Ventana/Roche, Ventana Medical Systems). The protocol used for the immunostainer was: dewaxing, antigen retrieval Cell Conditioning 1 (Ventana/Roche, Ventana Medical Systems) 36 min at 95°C, antibodies dilution following manufacturer's instruction for 32 min at 37°C, development in Ultra View Red staining (Ventana/Roche, Ventana Medical Systems, Inc., Tucson, USA) and counter-staining in Hematoxylin II (Ventana/Roche, Ventana Medical Systems, Inc., Tucson, USA). For Nestin, antigen retrieval was performed with microwave method at 100°C for 4 cicles 5 min each, in a citrate buffer solution (pH 6.0) and cooling for 20 min. Endogenous peroxidase activity was blocked with 3% H_2O_2 in absolute methanol for 10 min at room temperature (rt), in the dark. Antigen-antibody reaction was developed with the NovoLink Polymer Detection Kit (Novocastra, Newcastle, UK). Sections were incubated overnight in a wet chamber at 4°C with the antibodies for CD34, Nestin and WT1 (see Table 1 for technical details), then with NovoLink® Polymer for 30 min at rt, and finally with diaminobenzidine

(NovoLink® DAB Substrate Buffer) for 30 sec to 2 min. Cell nuclei were stained with Mayer's haematoxylin (Sigma Chemicals). Negative controls were done without the primary antibody. Finally, the dehydration samples were mounted onto glass slides using Canada Balsam (Sigma- Aldrich C1795). The obtained sections were observed under a light microscope (Leitz Wetzlak, Germany 12V max, 100W) connected with a charge-coupled device (CCD) camera Olympus CX42. Images were acquired using Image-Pro Plus software (Media Cybernetics http://www.mediacy.com) and processed with ImageJ free software (http://rsbweb.nih.gov/ij/).

Evaluation of microvessel density

The intraplaque neoangiogenesis was evaluated by CD34, and specific areas named region of interest (ROI) were assessed, which were defined as areas with CD34-positive neoangiogenesis. Afterwards, the microvessel counting was performed for CD34, Nestin and WT1 separately, as previously done on healthy tissue (Vasuri et al., 2012). Briefly, we divided each ROI in 1-mm^2 fields at 20x magnification, using a Olympus® ocular micrometer (1 length unit=5 μm, which means that an area of 100 x 100 units is equal to 0.25 mm^2). The Nestin- and WT1-positive vessels were counted in the same ROI where CD34 was evaluated.

The microvessel "density" of each antibody was obtained by dividing the sum of all positive structures observed in ROI by the number of the counted fields expressed in mm^2 (number of positive vessels/mm^2).

RNA extraction

The RNA was extracted from FFPE sections that had been stored for less than 6 months in a thermostatically controlled archival facility, at constant humidity, prior to RNA extraction. Depending on the specimen size, four to five 20-μm tissue slices were obtained for each sample under RNase free conditions. Then they were combined into a single nuclease-free screw cap tube. A commercial kit was used for RNA extraction (RNeasy® FFPE, Cat No. 74405, QIAGEN GmbH, Hilden, Germany); the protocol was slightly modified to increase RNA yield and purity. The samples were deparaffinized by adding twice xylene (800 μl) for 20 minutes with periodic vortexing plus ethanol (400 μl), followed by centrifugation for 5 min at 16 000 rpm and removal of the supernatant. The pellet was washed twice with 100% ethanol (1ml) followed by incubation for 2 min at RT and centrifugation for 2 min at 20 000 rpm. Residual ethanol was eliminated with SpeedVac centrifuge for 15min (UniEquip, Martinsried, Germany; model UNIVAPO 100H) equipped with a refrigerated aspirator vacuum pump, model Unijet II. For cell lysis, we added 20 μL of protease K, mixed by vortexing; the mixture was incubated for 30 min at 55°C, mixed at 850 rpm, then incubated again at 80°C for 15 min. Finally the RNA was eluted in 30 μl RNAse free-water, heated at 65°C for 5 min in order to be denatured and to inactivate Rnases, and stored at -80°C until used. RNA quality and concentration were measured by using an ND-1000 spectrophotometer (NanoDrop, Fisher Thermo, Wilmington, DE, USA). To compare the efficiency of RNA extraction from FFPE we used as a positive control RNA extracted from fresh tissue.

RT-PCR analysis

The reverse transcription assay was performed using 1.4 μg of total RNA per 25 μl of mix, following the manufacturer's protocol (High capacity cDNA Archive kit, Applied Biosystem). The cDNA was stored at -20°C until RT-PCR was performed. RT-PCR was carried out following MasterMix TaqMan® Protocol (TaqMan Univ PCR MasterMix, Applied Biosystems). Four μl of neat cDNA was amplified using specific probes for WT1 (NC_000011.9), Nestin (NC_000001.10) and βActin (NC_000007.13) in the RT-PCR mix (TaqMan® Gene Expression Assay, Applied Biosystems, respective ID assay: Hs01103751_m1, Hs04187831_g1, Hs 99999903_m1). Reactions were run on ABI PRISM 7900HT Sequence Detection System (Applied Biosystems). The cycling conditions were performed as follows: 10 min at 95°C, 50 cycles at 95°C for 15 s and 60°C for 60 sec. Each assay was carried out in triplicate and the transcription level was normalized using βActin as a reference gene (Cilloni et al., 2002). The threshold was set at 0.2 in order to be in the exponential phase. The expression values for atheromatous carotid plaques are presented as fold expression in relation to healthy arteries; the actual values were calculated using the $2-\Delta\Delta CT$ equation (Livak and Schmittgen, 2001), where $\Delta\Delta CT$ = [CT Target − CT βActin](atheromatous sample) − [CT Target − CT βActin] (healthy sample). Due to the technical difficulty to detect WT1 gene expression, Human immortalised myelogenous leukemia line cell line (K562) were used as a positive control

Table 1. Technical characteristics of the antibodies used.

Antibody	Clone	Dilution	Antigen retrieval	Manufacturer
CD34	Q-BEnd-10 (Mouse)	Pre-diluted	Cell Conditioning 1	Ventana, Roche, Tucson, USA
Nestin	10C2 (Mouse)	1:400	Citrate buffer, heat mediated	Millipore, Billerica, USA
WT1	6F-H2 (Mouse)	Pre-diluted	Cell Conditioning 1	Ventana, Roche, Tucson, USA

(Livak and Schmittgen, 2001; Cilloni et al., 2002; Ogawa et al., 2003; Kramarzova et al., 2012).

Statistical analysis

The statistics was performed using SPSS® ver. 20.0 software for Windows and Prism 5® software (GraphPad Software, Inc). Variables were expressed as means ± standard deviations (SD), ranges and frequencies. The differences between two groups (presence and absence of dot-like structures, AHA class V and class VI) were analyzed using the Mann-Whitney U test. The value of $P<0.05$ was considered significant. The RT-PCR data were analyzed assuming the null hypothesis that the threshold cycle (CT) differences between target and reference genes will be the same in atheromatous tissue vs healthy tissue. If the null hypothesis is not rejected, then the ΔΔCT would not be significantly different from 0, otherwise, the ΔΔCT can be derived from the estimation of the test. If a ΔΔCT is equal to 0 the ratio 2^-(ΔΔCT) will be 1, which indicates no differences in gene expression between control (healthy tissues) and pathological tissues (atheromatous tissues). All the P-values are derived from testing the null hypothesis that ΔΔCT are equal to 0 (at $P=0.05$). The SD and the confidence interval (CI) of 2^-(ΔΔCT) are all derived from the SD and CI of ΔΔCT as explained by Yuan et al. (2006).

Ethics

This study was carried out in conformity to the ethical guidelines of the 1975 Declaration of Helsinki (and following modifications), using surgical specimens sent to routine histological examination. Informed consent was obtained from all patients at the moment of surgery.

Results

Histological and immunohistochemical analysis of the neoangiogenetic component

The histological characteristics of the 49 examined

Table 2. Summary of the histological parameters evaluated in carotid plaque series.

Histological characteristics of the plaques examined (n=49)	
Mean minimum cap thickness (μm)	359.65±368.85 (40-1875)
Mean maximum cap thickness (μm)	946.16±468.76 (120-2125)
Lipid core extension	Absent: 4 cases (8.2%) 1/4: 10 cases (20.4%) 2/4: 13 cases (26.6%) 3/4: 16 cases (32.6%) 4/4: 6 cases (12.2%)
Calcification extension	Absent: 10 cases (20.4%) 1/4: 14 cases (28.6%) 2/4: 16 cases (32.6%) 3/4: 7 cases (14.3%) 4/4: 2 cases (4.1%)
Flogosis	Absent: 2 cases (4.1%) Mild: 10 cases (20.4%) Moderate: 11 cases (22.4%) Severe/Diffuse: 26 cases (53.1%)
Neoangiogenesis	Absent: 6 cases (12.2%) Focal: 12 cases (24.4%) Moderate: 14 cases (28.6%) Diffuse: 17 cases (34.8%)
AHA class VI	34 cases (69.4%)

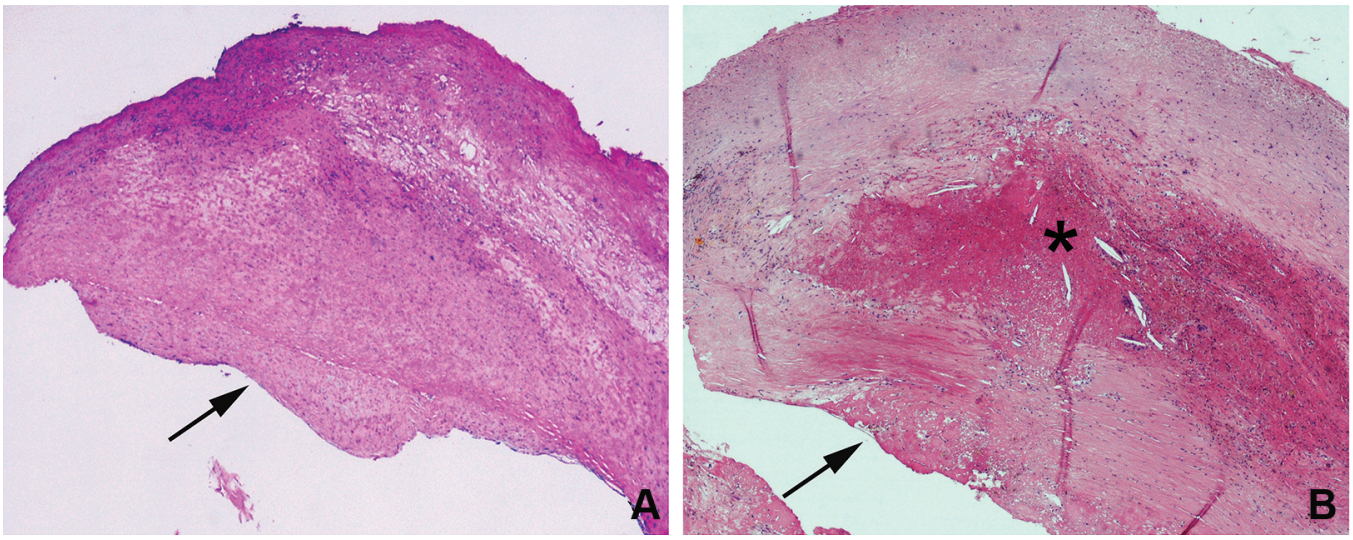

Fig. 1. A. An uncomplicated atheromatous plaque class V according to AHA. **B.** A complicated atheromatous plaque class VI according to AHA, with intra-plaque hemorrhage marked with a star. The arrows indicate the luminal surface. Haematoxylin-Eosin stain. x 4

plaques are listed in Table 2. Of note, 34 plaques (69.4%) were classified as AHA class VI (Fig. 1), due to the occurrence of hemorrhage in 26 cases (53.1%), erosion/ulceration in 16 cases (32.6%) and/or thrombosis in 3 cases (6.1%). The remaining plaques were classified as class V in 9 (18.4%) cases, class VII in 3 (6.1%), due to predominant calcification of the plaque core, and class VIII in 3 (6.1%), due to a predominant fibrotic change (Stary, 2000). Furthermore, 6 plaques (12.2%) showed no evidence of neoangiogenesis at histopathological examination, in line with what was previously reported by McCarthy et al. (1999). These 6 cases were excluded from the immunohistochemical analysis.

Table 3 summarizes the IHC results. At IHC, the mean number of CD34-positive neoangiogenetic structures in the 43 positive cases analyzed was 110.1±71.6 (range 11-283), the mean evaluated area was 2.6±1.6 mm^2 (range 0.3-8.3 mm^2), the mean final density of CD34-positive structures (obtained by dividing the sum of all positive structures by the mean evaluated area in mm^2) was 41.9±14.9/mm^2 (range 14.0-88.6/mm^2). The mean number of Nestin-positive structures was 64.0±46.5 (range 7-188), the mean evaluated area was 2.3±1.5 mm^2 (range 0.3-8.5 mm^2), the mean final density of Nestin-positive structures was 28.8±14.8/mm^2 (range 5.7-68.0/mm^2). The mean number of WT1-positive structures in the 43 cases analyzed was 42.3±41.4 (range 4-202), the mean evaluated area was 2.3±1.6 mm^2 (range 0.6-9.3 mm^2), the mean final density of WT1-positive structures was 17.7±11.4/mm^2 (range 4-52/mm^2).

We calculated the ratios between the mean densities of the three antibodies used in the analysis described above. The mean Nestin/CD34 density ratio was 0.68±0.24 (range 0.16-1.50), which means that 68% of the CD34-positive neovessels were positive for Nestin as well. This value is consistent with the 69% percentage that we found in normal *vasa vasorum* in our previous study on normal arteries (Vasuri et al., 2012). Conversely, the mean WT1/CD34 density ratio in our series was 0.42±0.22 (range 0.09-1.00), which means that 42% of CD34-positive neovessels were positive for WT1. This represents a lower percentage compared to normal arteries, where a mean of 63% of the *vasa vasorum* resulted to be WT1-positive. Finally, the mean WT1/Nestin ratio was 0.64±0.29 (range 0.17-1.33): in

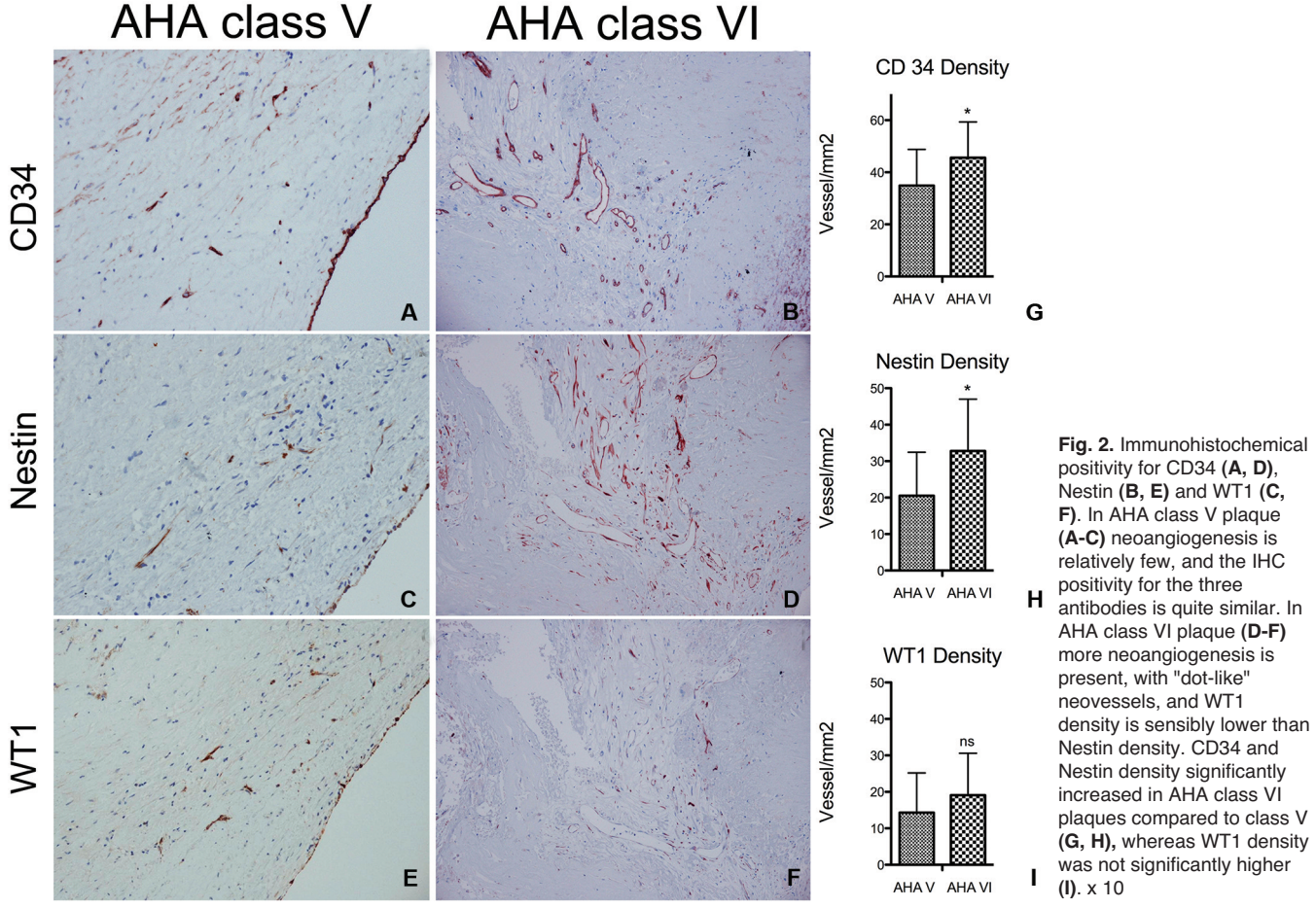

Fig. 2. Immunohistochemical positivity for CD34 **(A, D)**, Nestin **(B, E)** and WT1 **(C, F)**. In AHA class V plaque **(A-C)** neoangiogenesis is relatively few, and the IHC positivity for the three antibodies is quite similar. In AHA class VI plaque **(D-F)** more neoangiogenesis is present, with "dot-like" neovessels, and WT1 density is sensibly lower than Nestin density. CD34 and Nestin density significantly increased in AHA class VI plaques compared to class V **(G, H),** whereas WT1 density was not significantly higher **(I)**. x 10

Table 3. Immunohistochemical results of total cases and sorted by complicated / uncomplicated plaques (As stated in the text, 6 cases were excluded from the total series since they had no neoangiogenesis).

	Total (N=43)			Complicated Plaques (N=30)			Uncomplicated plaques (N=13)		
	CD34	Nestin	WT1	CD34	Nestin	WT1	CD34	Nestin	WT1
Mean evaluated area (mm^2)	2.6±1.6	2.3±1.5	2.3±1.6	2.8±1.6	2.4±1.6	2.5±1.7	2.1±1.5	1.9±1.4	1.8±1.1
N of positive vessels	110.1±71.6	64.0±46.5	42.3±41.4	127.2±70.1	73.0±40.7	47.4±41.6	75.4±60.5	46.2±55.0	31.5±41.1
Mean density (n of vessels/mm^2)	41.9±14.9	28.8±14.8	17.7±11.4	45.6±13.7	32.7±14.2	43.1±41.6	34.9±13.9	20.6±11.9	14.3±10.9

Table 4. Threshold cycle and 2^-(ΔΔCT) values for beta-actin, Nestin and WT1 (*p=0.001).

	CT values			2^-(ΔΔCT)	
	Beta-actin	Nestin	WT1	Nestin	WT1
Healthy arteries (n10)	35.8±4.6	30.1±1.9	39.3±2.6	1	1
Atheromatous arteries (n10)	35.3±3.0	32.9±3.8	42.6±4.2	0.1* (7 fold decrease)	0.05* (20 fold decrease)

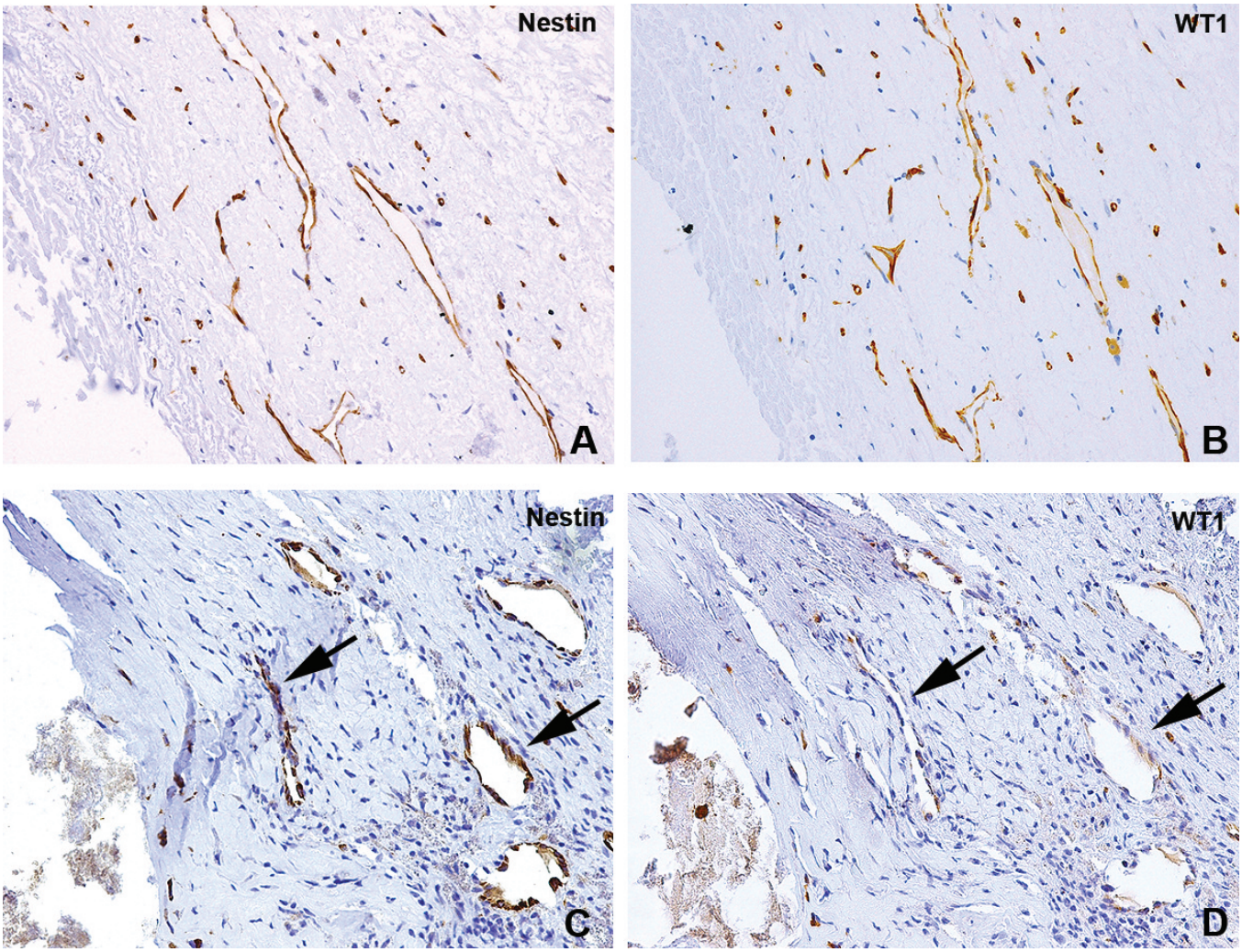

Fig. 3. Immunohistochemical staining for Nestin and WT1. **A.** Four vessels positive to Nestin and the same vessels positive to WT1 **(B)** (example of ratio 1:1). **C.** Five vessels positive to Nestin and the same vessels negative to WT1 **(D)**, representing the typical pattern Nestin +/WT1- (arrows). x 20

the *vasa vasorum* from normal arteries we reported a ratio close to 1.00 (i.e. *vasa vasorum* were Nestin+/WT+ or negative for both) (Vasuri et al., 2012), but in atherosclerotic plaques (Fig. 2) a subset of Nestin+/WT1- neovessels seems to exist.

In 18 cases out of 43 (41.9%), characterized by a high neoangiogenetic activity (high CD34 density, P=0.004, Mann-Whitney test), we observed foci of several "dot-like" capillary structures, i.e. single-cell CD34-positive structures without a visible lumen. These "dots" showed a strong immunoreactivity for Nestin (13/18 cases, 72.2%), but only a focal and weak reaction (or negativity) for WT1 (with only 2/18 diffusely positive cases, 11.1%). In all cases the Nestin+/WT1- neovessels were intermingled with neovessels with the complete phenotype (Nestin+/WT1+), without any preferential localization.

Relationship between the neoangiogenesis phenotype and plaque instability

To assess whether phenotypic neoangiogenic profile is linked to the occurrence of plaque histopathological complications, we correlated the IHC density profiles with the AHA class (Table 3). In plaques diagnosed as class V, VII or VIII (n=13) the mean CD34 density was 34.9±13.9, the mean Nestin density was 20.6±11.9, the mean WT1 density was 14.3±10.9 (Fig. 2A-C), with no differences among classes. In plaques diagnosed as class VI (n=30) mean CD34 density was 45.6±13.7, mean Nestin density was 32.8±14.2, mean WT1 density was 19.1±11.6 (Fig. 2D-F). CD34 and Nestin neovessel densities increased significantly in patients presenting class VI plaques (P=0.045 and P=0.009 respectively, Mann-Whitney test), while the WT1 neovessel density was not significantly different between class VI plaques and uncomplicated plaques (P=0.139, Fig. 2G-I). Complicated atheromatous plaques seem to be related not only to neoangiogenesis (CD34+ density), but also with the occurrence of the Nestin+/WT1- neoangiogenic profile.

RT-PCR analysis

WT1 and Nestin mRNA were analyzed in all the 20 samples. The total mean extracted mRNA from healthy or atheromatous tissue was 1129.8 ng (range 322.5-1815.8) and 1147.1 (range 620.5-2232.0) ng respectively. Results are listed in table 4. The mean CT values of endogenous control (β-Actin) was 35.8 (SD 4.6, CI 34.1-37.5) in healthy tissue and 35.3 (SD 3.0, CI 34.1-36.5) in atheromatous tissue. Mean CT for tested gene Nestin and WT1 were respectively 30.1 (SD 1.9, CI 29.4-30.8) and 39.3 (SD 2.6, CI 38.3-40.3) in healthy tissue, and 32.9 (SD 3.8, CI 31.5-34.4) and 42.6 SD 4.2, CI 40.9-44.1) in atheromatous tissue. A mean CT value of 38.0 was obtained for K562 cell line positive control for WT1. Additionally, a mean of CT=38.7 was also obtained in the atheromatous fresh tissue control. These high CT values for WT1 gene expression are compatible with the small amounts of WT1 transcript present in tissue and with the CT values reported in the literature (Cilloni et al., 2002; Ogawa et al., 2003; Kramarzova et al., 2012). Indeed WT1 expression was considered negative if the subject scored CT >50 repeatedly (Cilloni et al., 2002). None of our samples were negative for WT1 expression. ΔΔCT Nestin and ΔΔCT WT1 were significantly different from 0 (P=0.035 and P=0.029 respectively), thus the null hypothesis was rejected, which indicated a change in Nestin and WT1 gene expression between healthy and atheromatous tissues. In atheromatous tissue, the mean ΔΔCT Nestin was 2.8 (SD 1.4, CI 1.8-3.9) and the mean ΔΔCT WT1 was 4.4 (SD 1.7, CI 2.8-5.9). This corresponds to 2^-(ΔΔCT) of 0.1 for nesting gene expression (SD: 2^-(1.4), CI (2^-1.8-2^-3.9) and 0.05 for WT1 gene expression in atheromatous plaques (SD: 2^-(1.7), CI (2^-2.8 – 2^-5.9). The atheromatous tissue showed a 7-fold expression decrease for Nestin gene and a 20-fold expression decrease for WT1 gene compared to controls. WT1 gene expression is reduced more than 3 times (p=0.001) compared to Nestin gene expression in atherosclerotic tissues.

Discussion

Neoangiogenesis is a key event in atheromatous plaque formation and progression, and its involvement in intra-plaque complications (hemorrhage and rupture) has been demonstrated (Mofidi et al., 2001; Moreno et al. 2006; Hermus et al., 2010; Faggioli et al., 2011). According to the literature, the main source for neoangiogenesis in diseased arteries is the proliferation of *vasa vasorum*, and in particular of the second-order *vasa vasorum* located in the adventitia (Kwon et al., 1998; Mulligan-Kehoe, 2010). In a previous paper from our group (Vasuri et al., 2012), we observed that *vasa vasorum* from adult healthy arteries express Nestin and WT1 with a 1:1 ratio. In the present work we studied the same vascular markers in atheromatous plaques, and we found that intra-plaque neovessels still expressed both Nestin and WT1, but this Nestin+/WT1+ phenotype was represented only in 64% of the neovessels, while the remaining showed a Nestin+/WT1- phenotype. Another consideration is that "dot-like" neovessel structures were observed in atheromatous plaques with active neoangiogenesis: these small structures strongly expressed CD34 and Nestin, but weakly expressed WT1, thus exhibiting the Nestin+/WT1- phenotype. Due to their correlation with CD34 density, these "dot-like" neovessels are likely to represent the growth edge of the plaque neovascularization, with a distinctive Nestin+/WT1- profile.

Our PCR analysis, conducted on 10 plaques of our series, as well as 10 healthy control arteries, showed a 7-fold decrease in Nestin mRNA in plaques, but a 20-fold decrease in WT1 mRNA, which confirms the IHC evidence that in atheromatous plaques Nestin can also be

expressed in the absence of WT1. In 2005, a first study showed a decreasing or total absence of WT1 expression in the endothelium in vascular malformations (Lawley et al., 2005). Five years later a larger study involving 126 cases of vascular tumors and 30 cases of vascular malformations confirmed the absence of WT1 protein in the endothelium of vascular malformations (Al Dhaybi et al., 2010). WT1 mRNA is expressed at very low concentration in the tissue, thus the difficulty to detect it by RT-PCR (Cilloni et al., 2002); of note, here we succeeded in detecting WT1 mRNA from FFPE arterial samples. In addition to vascular malformations, here we showed that both WT1 protein and particular WT1 mRNA expression significantly decreased in neovessels of atherosclerotic lesions compared to healthy arteries. This phenotype may be explained by defects in WT1 signalling which, as in vascular malformations, may underlie the inability of endothelial cells to undergo physiologic apoptosis. The finding that Nestin mRNA is decreased in diseased arteries compared to normal specimens can be questioned, since the neoangiogenesis in plaques is supposed to be Nestin-positive: a possible explanation of this phenomenon is that at IHC we evaluated only specific CD34-positive ROI, and only the diseased intima obtained by endarterectomy was available for IHC and PCR analysis. Conversely, in normal specimens, the whole vessel wall was evaluated, including the adventitial *vasa vasorum*.

Which events might be able to unleash the Nestin+/WT1- phenotype in neovessels of atheromatous plaques is quite an interesting issue that deserves further investigation. A possible hypothesis is that the quickly-proliferating vessels might lose the negative growth control by means of WT1. Recently, the implication of WT1 in the vascular response to myocardial ischemia and its oncogenic potential was seen as a promoter of tumor angiogenesis (Scholz et al., 2009). Indeed, angiogenesis is regulated by the balance between two splice-isoforms of VEGF: the pro-angiogenic VEGF(165) and the anti-angiogenic VEGF(165)b. Eventual WT1 mutations suppress the anti-angiogenic effects of VEGF(165)b in tumors (Amin et al., 2011). Our results are likely to suggest that a decrease of WT1 leads to a loss of repression (or regulation) on neoangiogenesis as in tumors, thus leading to an abnormal neovascularization.

Moreover, a noteworthy result is the finding that Nestin+/WT1- neoangiogenesis is linked to the occurrence of intra-plaque histopathological complications, at least in our series: in uncomplicated plaques (class V, VII, and VIII according to Stary 2000) and complicated plaques (class VI), the density of Nestin-positive structures rises from 20.5/mm^2 to 32.8/mm^2, respectively (P=0.009), while the difference in the density of WT1-positive structures (14.3/mm^2 and 19.1/mm^2) is minor and not significant (P=0.139). While the relationship between the amount of neoangiogenesis and plaque instability is well established (Moreno et al., 2006), our results seem to suggest that the phenotypic switch that leads to Nestin+/WT1 -neoangiogenesis occurs in advanced plaques, and it might be involved in the development of the so-called vulnerable plaque. One hypothesis is that Nestin+/WT1- neovessels might represent the final expression of a rapidly growing neoangiogenesis, with the "dot-like" structures as the growing edge. This rowdy neoangiogenesis could be constituted by immature, fragile vessels, prone to rupture (McCarthy et al., 1999; Sluimer et al, 2009). This could also explain the prevalence of the Nestin+/WT1- phenotype in plaques with high neoangiogenesis, as well as its relationship with the occurrence of the histopathological complications included in AHA class VI (i.e. hemorrhage, rupture, etc.).

One possible limitation of the present study might be represented by the sample size (n=49), imposed by the surgical activity of our Institution. In any case, we surmise that the distribution of the variables between the two groups of plaques are adequate for our preliminary data, and therefore that our series is quite representative of the described phenomenon. Another questionable issue is the comparison between the carotid plaques (where only the diseased intima and the inner media layers are available for analysis) and the healthy arteries (where the whole vessel wall is present, including adventitia), which we already mentioned above. Thus, it should be kept in mind that our purpose was not to evaluate the "global" expression of Nestin and WT1 in the whole vessels, but to evaluate the relationship existing between the two transcripts. The RT-PCR results are likely to confirm what was observed at IHC. At any rate, although it is plausible that intra-plaque neoangiogenesis may derive from *vasa vasorum*, we do not exclude different origins (e.g. circulating progenitor cells), and the different Nestin+/WT1- phenotype would also fit anyway with these different hypotheses.

In conclusion, within the atheromatous lesions Nestin-driven neoangiogenesis might be activated by alternative transcription factors other than WT1, giving rise to a Nestin+/WT1- phenotype, together with the Nestin+/WT1+ phenotype. Furthermore, these Nestin+/WT1- neovessels are significantly more represented in AHA class VI than in plaques of other classes, and they are therefore associated with plaque vulnerability. This represents a starting point for our ongoing studies, since the identification of new transcription factors, and the possibility of their regulation in future, can open new perspectives in the therapeutic approach of vulnerable atheromatous plaques.

References

Al Dhaybi R., Powell J., McCuaig C. and Kokta V. (2010). Differentiation of vascular tumors from vascular malformations by expression of Wilms tumor 1 gene: evaluation of 126 cases. J. Am. Acad. Dermatol. 63, 1052-1057.

Amin E.M., Oltean S., Hua J., Gammons M.V., Hamdollah-Zadeh M., Welsh G.I., Cheung M.K., Ni L., Kase S., Rennel E.S., Symonds

K.E., Nowak D.G., Royer-Pokora B., Saleem M.A., Hagiwara M., Schumacher V.A., Harper S.J., Hinton D.R., Bates D.O. and Ladomery M.R. (2011). WT1 mutants reveal SRPK1 to be a downstream angiogenesis target by altering VEGF splicing. Cancer Cell. 20, 768-780.

Cilloni D., Gottardi E., De Micheli D., Serra A., Volpe G., Messa F., Rege-Cambrin G., Guerrasio A., Divona M., Lo Coco F. and Saglio G. (2002). Quantitative assessment of WT1 expression by real time quantitative PCR may be a useful tool for monitoring minimal residual disease in acute leukemia patients. Leukemia. 16, 2115-2121.

Faggioli G.L., Pini R., Mauro R., Pasquinelli G., Fittipaldi S., Freyrie A., Serra C. and Stella A. (2011). Indentification of carotid "vulnerable plaque" by contrast-enhanced iltrasonography: correlation with plaque histology, symptoms and cerebral computed tomography. Eur. J. Vasc. Endovasc. Surg. 41, 238-248.

Hermus L., Tiellu I.F., Wallis deVries B.M., van der Dungen J.J. and Zeebregts C.J. (2010). Imaging the vulnerable carotid artery plaque. Acta. Chir. Belg. 110, 159-164.

Hobson R.W. 2nd, Mackey W.C., Ascher E., Murad M.H., Calligaro K.D., Comerota A.J., Montori V.M., Eskandari M.K., Massop D.W., Bush R.L., Lal B.K. and Perler BA. (2008). Management of atherosclerotic carotid artery disease: clinical practice guidelines of the Society for Vascular Surgery. J. Vasc. Surg. 48, 480-486.

Hohenstein P. and Hastie N.D. (2006). The many facets of the Wilms' tumour gene, WT1. Hum. Mol. Genet. 15, R196-201.

Kramarzova K., Stuchly J., Willasch A., Gruhn B., Schwarz J., Cermak J., Machova-Polakova K., Fuchs O., Stary J., Trka J. and Boublikova L. (2012). Real-time PCR quantification of major Wilms' tumor gene 1 (WT1) isoforms in acute myeloid leukemia, their characteristic expression patterns and possible functional consequences. Leukemia 26, 2086-2095.

Kullo I.J., Edwards W.D. and Schwartz R.S. (1998). Vulnerable plaque: pathobiology and clinical implications. Ann. Intern. Med. 129, 1050-1060.

Kumamoto M., Nakashima Y. and Sueishi K. (1995). Intimal neovascularization in human coronary atherosclerosis: its origin and pathophysiological significance. Hum. Pathol. 26, 450-456.

Kwon H.M., Sangiorgi G., Ritman E.L., McKenna C., Holmes D.R. Jr, Schwartz R.S. and Lerman A. (1998). Enhanced coronary *vasa vasorum* neovascularization in experimental hypercholesterolemia. J. Clin. Invest. 101, 1551-1556.

Lawley L.P., Cerimele F., Weiss S.W., North P., Cohen C., Kozakewich H.P., Mulliken J.B. and Arbiser J.L. (2005). Expression of Wilms tumor 1 gene distinguishes vascular malformations from proliferative endothelial lesions. Arch. Dermatol. 10, 1297-1300.

Liapis C.D., Bell P.R., Mikhailidis D., Sivenius J., Nicolaides A., Fernandes e Fernandes J., Biasi G. and Norgren L. (2009). ESVS guidelines. Invasive treatment for carotid stenosis: indications, techniques. Eur. J. Vasc. Endovasc. Surg. 37 (4 Suppl), 1-19.

Livak K.J. and Schmittgen T.D. (2001). Analysis of relative gene expression data using real-time quantitative PCR and the 2(-Delta Delta C(T)) Method. Methods. 25, 402-408.

McCarthy M.J., Loftus I.M., Thompson M.M., Jones L., London N.J., Bell P.R., Naylor A.R. and Brindle NP. (1999). Angiogenesis and the atherosclerotic carotid plaque: an association between symptomatology and plaque morphology. J. Vasc. Surg. 30, 261-268.

Mofidi R., Crotty T.B., McCarthy P., Sheehan S.J., Mehigan D. and Keaveny T.V. (2001). Association between plaque instability, angiogenesis and symptomatic carotid occlusive disease. Br. J. Surg. 88, 945-950.

Moreno P.R., Purushothaman K.R., Zias E., Sanz J. and Fuster V. (2006). Neovascularization in human atherosclerosis. Curr. Mod. Med. 6, 457-477.

Mulligan-Kehoe M.J. (2010). The *vasa vasorum* in diseased and nondiseased arteries. Am. J. Physiol. Heart. Circ. Physiol. 298, H295-H305.

Ogawa H., Tamaki H., Ikegame K., Soma T., Kawakami M., Tsuboi A., Kim E.H., Hosen N., Murakami M., Fujioka T., Masuda T., Taniguchi Y., Nishida S., Oji Y., Oka Y. and Sugiyama H. (2003). The usefulness of monitoring WT1 gene transcripts for the prediction and management of relapse following allogeneic stem cell transplantation in acute type leukemia. Blood. 101, 1698-1704.

Ramasamy K., Dwyer-Nield L.D., Serkova N.J., Hasebroock K.M., Tyagi A., Raina K., Singh R.P., Malkinson A.M. and Agarwal R. (2011). Silibinin Prevents Lung Tumorigenesis in Wild-Type but not in iNOS–/– Mice: Potential of Real-Time Micro-CT in Lung Cancer Chemoprevention Studies. Clin. Cancer. Res. 17, 753-761.

Scholz H., Wagner K.D. and Wagner N. (2009). Role of the Wilms' tumour transcription factor, Wt1, in blood vessel formation. Pflugers. Arch. 458, 315-323.

Sluimer J.C., Kolodgie F.D., Bijnens A.P., Maxfield K., Pacheco E., Kutys B., Duimel H., Frederik P.M., van Hinsbergh V.W., Virmani R. and Daemen MJ. (2009). Thin-walled microvessels in human coronary atherosclerotic plaques show incomplete endothelial junctions relevance of compromised structural integrity for intraplaque microvascular leakage. J. Am. Coll. Cardiol. 53, 1517-1527.

Stary H.C. (2000). Natural history and histological classification of atherosclerotic lesions. An update. Arterioscler. Thromb. Vasc. Biol. 20, 1177-1178.

Stary H.C., Chandler A.B., Dinsmore R.E., Fuster V., Glagov S., Insull W. Jr, Rosenfeld M.E., Schwartz C.J., Wagner W.D. and Wissler R.W. (1995). A definition of advanced types of atherosclerotic lesions and a histological classification of atherosclerosis. Arterioscler. Thromb. Vasc. Biol. 15, 1512-1531.

Teranishi N., Naito Z., Ishiwata T., Tanaka N., Furukawa K., Seya T., Shinji S. and Tajiri T. (2007). Identification of neovasculature using nestin in colorectal cancer. Int. J. Oncol. 30, 593-603.

Vasuri F., Fittipaldi S., Buzzi M., Degiovanni A., Stella A., D'Errico-Grigioni A. and Pasquinelli G. (2012). Nestin and WT1 expression in small-sized *vasa vasorum* from human normal arteries. Histol. Histopathol. 27, 1195-1202.

Wagner N., Wagner K.D., Scholz H., Kirschner K.M. and Schedl A. (2006). Intermediate filament protein nestin is expressed in developing kidney and heart and might be regulated by the Wilms' tumor suppressor Wt1. Am. J. Physiol. Regul. Integr. Comp. Physiol. 291, R779-787.

Wagner N., Panelos J., Massi D. and Wagne K.D. (2008). The Wilms' tumor suppressor WT1 is associated with melanoma proliferation. Pflugers. Arch. 455, 839-847.

Yuan J.S., Reed A., Chen F. and Stewart C.N. Jr (2006). Statistical analysis of real-time PCR data. BMC Bioinformatics 7, 85.

Accepted May 26, 2014